Article:

Impulse Magnetised Magnetic Screws

Hany M. Mohamed, Kais Atallah

Department of Electronic and Electrical Engineering, University of Sheffield, Sheffield, U.K.

Abstract— **the paper is an investigation in the performance of two types magnetic screws (MSs). The first is the magnet-to-magnet and consists of permanent magnet (PM) nut and PM screw and the second is a magnet-to-reluctance and consists of PM nut and a double start reluctance screw (RS). It is argued, that for cost sensitive and long stoke applications, a magnet-to reluctance MS may be the preferred option. It is also shown that capacitor discharge magnetisation techniques can be employed for imprinting helical magnetisation distributions on cylindrical PMs, significantly reducing complexity and facilitating the practical realisation of MS systems.**

Index Terms—**Magnetic screw, impulse magnetisation.**

I. INTRODUCTION

S imilar to the mechanical counterparts, MSs convert rotary motion to linear motion and vice-versa. They enable the realisation of linear electrical machine topologies, employing a rotary electrical machine as prime-mover, while achieving overall force densities significantly higher than those of conventional linear electrical machines. Therefore, they have been considered for many applications, such as wave energy converters [1], artificial hearts [2] and vehicle active suspension [3]. However, the practical realisation of the helical magnetisation distribution on the PM screw and/or the PM nut remains a challenge, and several methods using discrete PM pieces have been proposed [4, 5].

In the paper, a MS consisting of PM nut and a double start RS is presented. Its performance is compared to MSs having PM nut and PM screw, and it is shown that for long stroke dynamic applications, in particular, it would be the preferred solution, due to the reduction in PM usage and the inherently smaller inertia of the RS, which results in lower torque/power requirements of the prime-mover rotary machine in highly dynamic applications. The effects of leading design parameters, such as the length of the air-gap, the lead of the screw and thickness of the PMs on the force transmission capability of the MS is presented and discussed. Furthermore, for the manufacture of the PM nut, it is proposed to employ capacitor discharge impulse magnetisation with a specifically developed double-sided magnetising fixture to imprint helical magnetisation distribution on radially anisotropic cylindrical PMs. It is shown that impulse magnetisation techniques can facilitate the realisation of MSs, making them viable options for many applications. A MS with a 10mm lead, is designed and

prototyped and a special test-rig is developed to measure the relationship between the angular and linear displacements and the transmitted force.

II. MAGNETIC SCREWS

Investigation of the force transmission capability is undertaken for two types of MSs, magnet-to-magnet and magnet-to-reluctance types. In the analysis the inner diameter of the nut is fixed at 16mm.

A. Magnet-to-magnet MS

A schematic of a magnet-to-magnet type MS is shown in Fig. 1, where the helically magnetised PMs are mounted on the nut and screw. The effect of different magnet dimensions, pole-pitch, lead, and air-gap length are investigated.
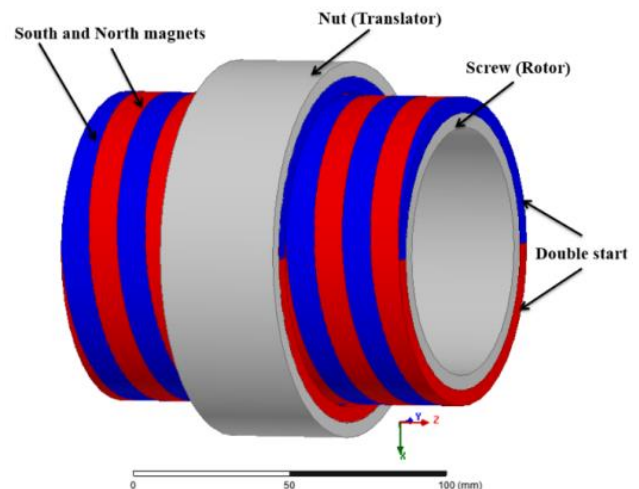

Fig. 1. Two-pole double start magnet-to-magnet type MS.

Magnet thickness has a significant effect on the magnetic field produced by a magnet and, hence, affecting the force/shear stress transmitted by a MS. The investigation is undertaken for a fixed air-gap nut bore diameter. For a 1 mm air-gap, and for a nut equipped with a single lead, Fig. 3 shows the variations of the air-gap shear stress with the lead length for different PM thicknesses. It can be seen that, for a given PM thickness a lead length exists for which the air-gap shear stress is maximum. Fig. 4 shows the variation of maximum shear stress with PM thickness, it can be seen that the rate of increase in maximum shear stress with PM thickness decreases with increasing PM

thickness. Accordingly, an optimum magnet thickness should be selected as a trade-off between force transmission and cost.
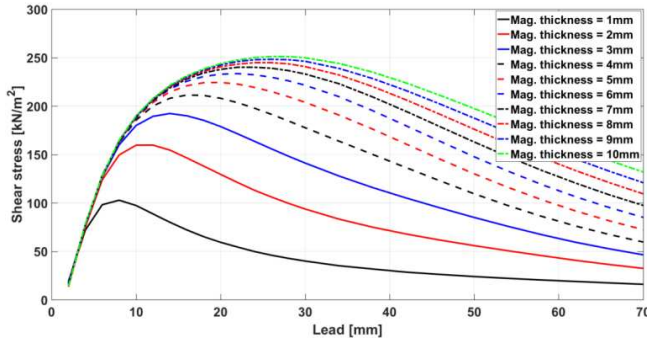

Fig. 1. Variation of shear stress with lead for different magnet thickness. (1mm airgap)

The effect of changing the air-gap length on shear stress is also investigated. For a constant lead, the variation of shear stress with air-gap length at different PM thicknesses is shown in Fig. 5.
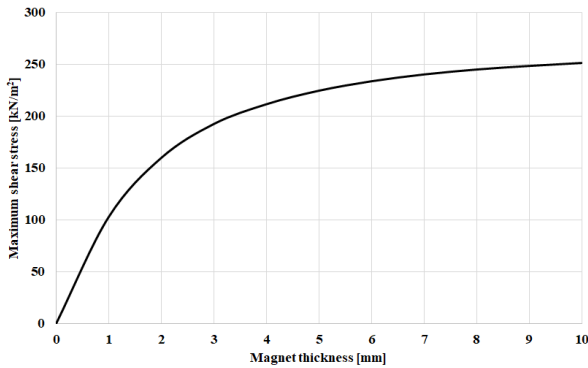

Fig. 2. Variation of maximum shear stress with PM thicknesses for magnet-to-magnet MS.

It can be seen that the air-gap length has a significant effect on the shear stress and for a given magnet thickness shear stress decreases with increasing the air-gap. It can also be seen that for a given air-gap length increasing the PM thickness beyond a certain value results in negligible increase in shear stress. However, as it is always the case, the selection of the air-gap length is trade-off between the magnetic performance, cost, and practical realisation.
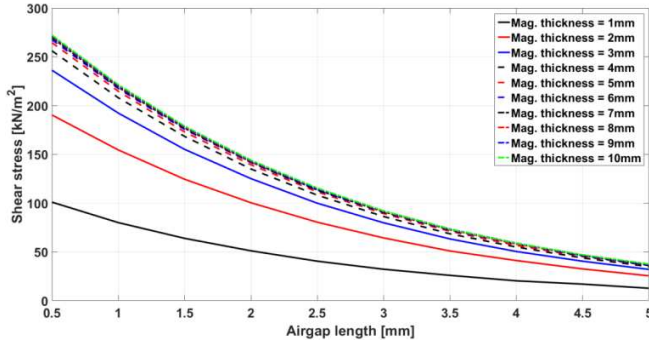

Fig. 3. Variation of shear stress with air-gap length at different PM thicknesses. (14mm lead)

B. Magnet-to-reluctance MS

For a magnet-to-reluctance type MS, magnetic poles on the screw (rotor) are replaced by iron threads as shown in Fig. 6. Replacing the PMs on the screw, results in lower thrust force, however, production and material costs are also reduced.

Similarly, effects of changing the dimensions of iron threads, and air-gap on the shear stress are investigated.
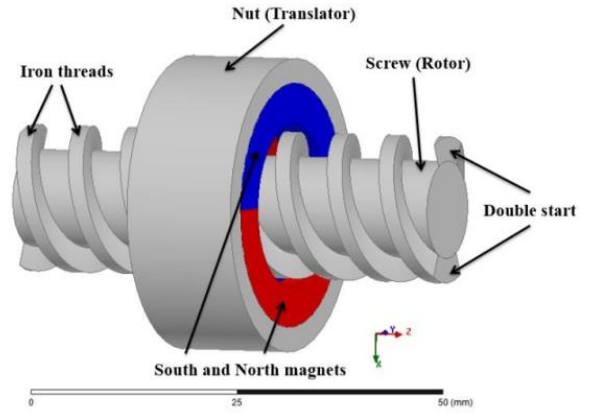

Fig. 4. Two-pole double start magnet-to-reluctance type MS.

The effect of the dimensions of iron thread on shear stress is investigated. In the analysis, the PM thickness and the air-gap diameter are fixed. Two main parameters characterise the screw, the width of the iron thread as percentage of pole-pitch, and the depth of the thread. Fig. 7 shows the variation of shear stress with iron thread width for different iron thread depth at fixed PM thickness.
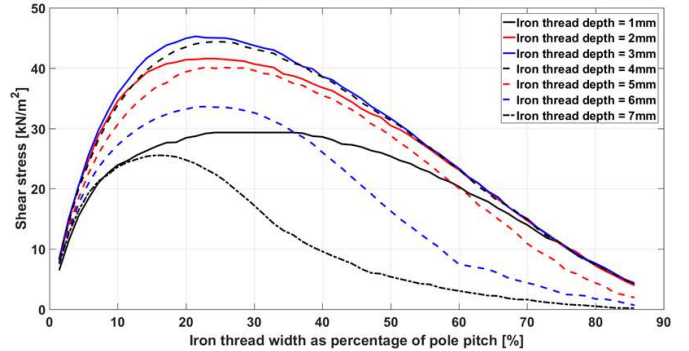

Fig. 5. Variation of shear stress with iron thread width at fixed magnet thickness. (3mm magnet thickness, 1mm airgap length and 14mm lead)

Thus for the particular PM thickness, results show that an iron thread width between 20 % and 30 % of pole-pitch and iron thread depth of 3 mm should be selected for maximum shear stress. The maximum shear stress achieved at different air-gap lengths is shown in Fig. 8. Clearly, airgap length has a
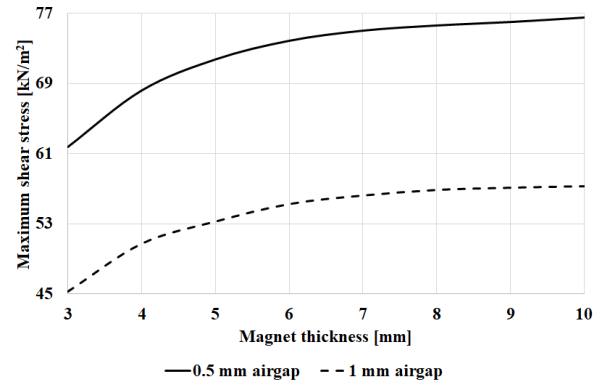

Fig. 6. Variation of maximum shear stress with magnet thickness for different air-gap lengths. (14mm lead)

significant effect, and there is a magnet thickness beyond which increase in shear stress is not significant.

In spite of higher thrust force gained from magnet-to-magnet MS, reluctance type MS may be preferred in cost sensitive and long stroke applications. Simplicity of the screw design and the reduced use of PM material, which is confined to the nut, makes this topology a good candidate for many applications. However, because the screw is made of solid mild steel, the losses and efficiency need to be carefully assessed, and simulation studies have been undertaken. The dominant losses are eddy currents in screw and to a lesser extent in magnets and the back-iron of the nut. In the analysis, the simultaneous rotary and linear motions of the screw and the nut, respectively, are applied, Fig. 9, and 3D finite element analysis (FEA) is employed. Fig. 10 shows the variation of the losses with the speed of the nut. It can be seen that the load condition doesn't have a significant effect on the losses. Fig. 11, show the efficiency map, where it can be seen that efficiencies in of 99% can be achieved.
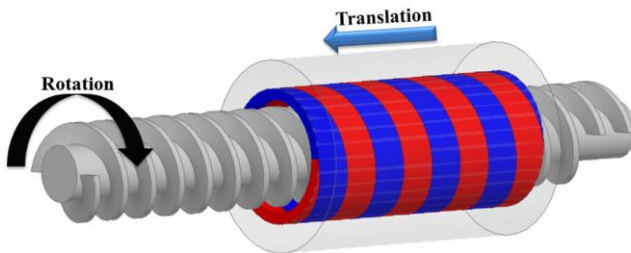

Fig. 9 Simultaneous motions of the screw and nut for loss predictions employing FEA. (design subsequently prototyped)
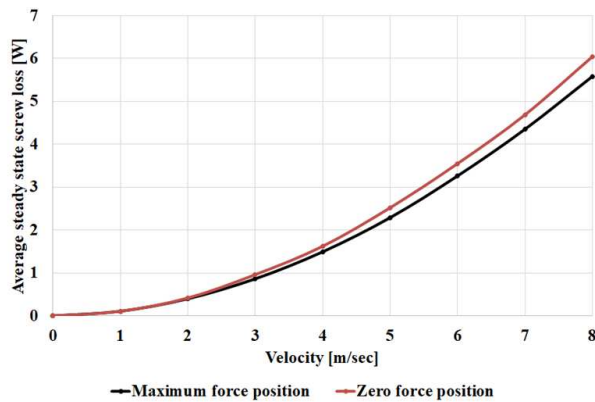

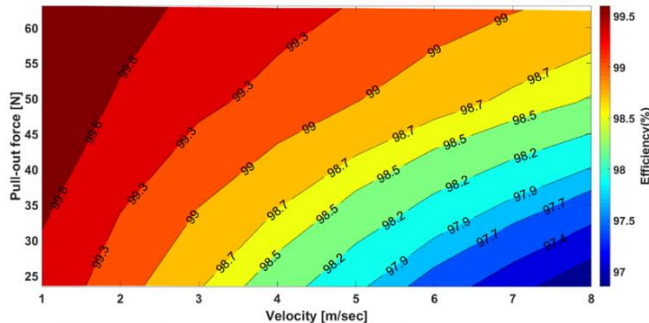Fig. 10 Variation of eddy current losses with speed of the nut.


Fig. 11 Efficiency map.

III. EXPERIMENTAL INVESTIGATION

A double sided single conductor magnetising fixture is employed to imprint a helical magnetization having a 10mm lead on 40mm long nut, realised from 5 axially stacked radially anisotropic NdFeB ring PMs. The ring PMs have inner and outer diameters of 16mm and 19mm, respectively, and axial length of 8mm. The windings are wound around the fixture in a helical configuration to generate a helically shaped magnetic field distribution. Fig. 12, shows the inner part of the magnetising fixture, where the helically shaped winding is wound in the groove of a double start mild steel screw. The outer part is wound in helical slots machined in a Tufnol piece assembled from 2 halves. Fig. 13 shows the assembled fixture prior to the magnetization of the PMs. Fig. 14, shows the simulated flux density distribution in the nut at the peak current flowing through the fixture, where flux densities in excess of 3.5T can be achieved. Using a magnetic field viewing film, Fig. 15 shows the helical pattern imprinted on the nut.

The magnetised PMs are used to produce a magnet-to-reluctance screw, and a test-rig was developed to measure the relationship between the linear and rotary displacements and the transmitted force. On no-load, Fig. 16 shows the variation of the linear movement of the screw with the rotary movement of the nut. It can be seen the relationship is linear and agrees with predictions.

In order to take into consideration of the fact that due to the short pole-pitch and the strong axial component of the magnetizing field, not all the magnet would fully magnetised in
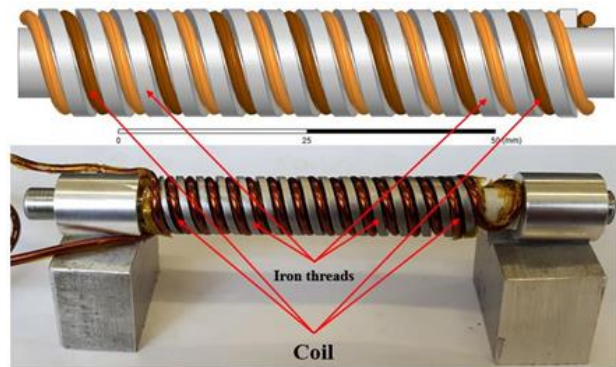
(a) Before fibre glass banding
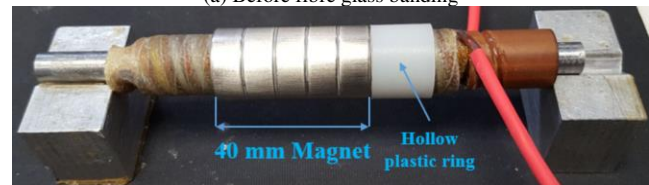
(b) After fibreglass banding and magnet insertion
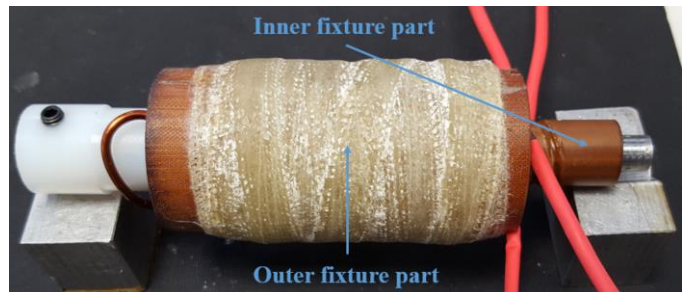Fig. 12 Inner part of single conductor double-sided fixture.

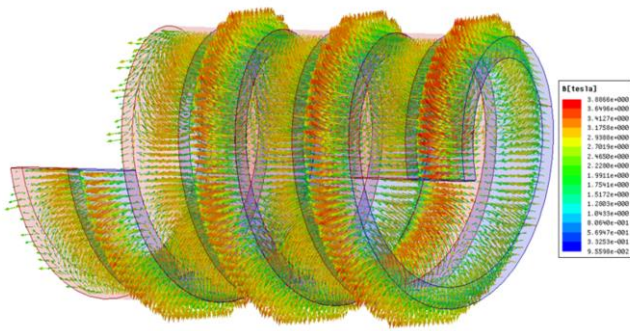Fig. 13 Assembled magnetizing fixture with overall fiberglass banding.

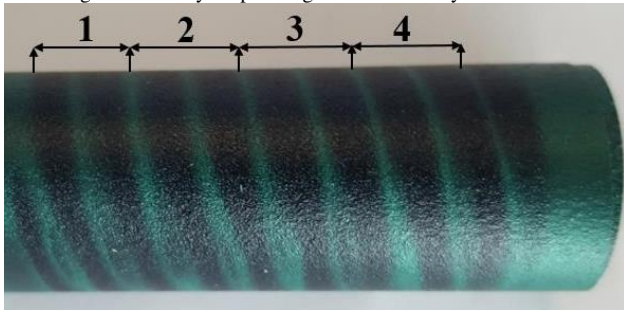Fig. 14 Helically shaped magnetic flux density distribution.

Fig. 15 The 40 mm helically magnetised cylindrical magnet with its 4 pole-pairs.

the radial direction, the force produced by the experimental magnet-reluctance screw is simulated by sub-dividing the magnets into regions, each with specific estimated equivalent remanence. Fig. 17 compares measured and predicted transmitted force. In order to minimize the effects of friction on the measurement, two methods are employed. In method 1, as the nut is rotated at specific angles, the screw is constrained using a load cell. In this case friction will reduce the measured value. In method 2, the screw is held in a vertical position and loaded with calibrated weights, and the new stable position is recorder. For this case friction acts with the transmitted force. It can be seen, that despite the uncertainties associated with the extent of full magnetization in the nut, the results seem confirm the prediction. Fig. 18 shows a picture of the test-rig for force measurement, using method 1 and 2.

IV. CONCLUSION

The force transmission capabilities of magnet-to-magnet and magnet-to-reluctance magnetic screws are investigated. It has been shown that although magnet-to-magnet topology exhibits a significantly higher force/torque transmission capability, a magnet-to-reluctance magnetic screw can be a good candidate for cost sensitive and long stroke applications. Furthermore, although the realisation of helical magnetization distribution has realised using discrete magnet pieces, it has been shown that impulse magnetisation techniques can be used for imprinting helical magnetisation distributions on cylindrical magnets, resulting in simpler and cost-effective manufacturing techniques.

REFERENCES

[1] R. K. Holm, N. I. Berg, M. Walkusch, P. O. Rasmussen, and R. H. Hansen, "Design of a Magnetic Lead Screw for Wave Energy Conversion," *IEEE Transactions on Industry Applications,* vol. 49, pp. 2699-2708, 2013.

[2] J. Ji, Z. Ling, J. Wang, W. Zhao, G. Liu, and T. Zeng, "Design and Analysis of a Halbach Magnetized Magnetic Screw for Artificial Heart," *IEEE Transactions on Magnetics,* vol. 51, pp. 1-4, 2015.

[3] N. I. Berg, R. K. Holm, and P. O. Rasmussen, "A novel magnetic lead screw active suspension system for vehicles," in *2014 IEEE Energy Conversion Congress and Exposition (ECCE)*, 2014, pp. 3139-3146.

[4] Z. Ling, J. Ji, J. Wang, and W. Zhao, "Design Optimization and Test of a Radially Magnetized Magnetic Screw With Discretized PMs," *IEEE Transactions on Industrial Electronics,* vol. 65, pp. 7536-7547, 2018.

[5] F. Gao, Q. Wang, Y. Hu, B. Chen, B. Zhao, and J. Zou, "Performance Evaluation of Magnetic Lead Screws Equipped With Skewed Arc Magnets Instead of Helical Ones," *IEEE Transactions on Magnetics,* pp. 1-5, 2018.
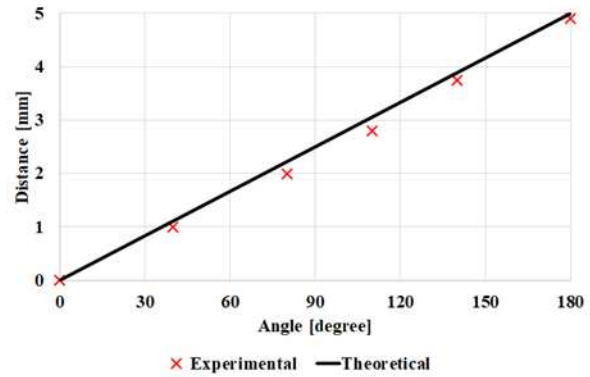
Fig. 16 Variation of linear displacement with rotary displacement at no load.
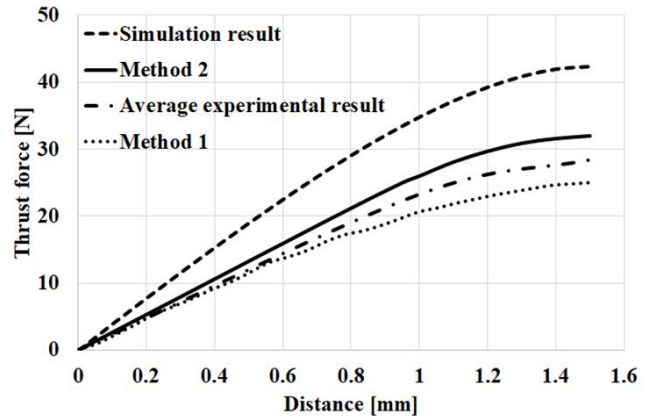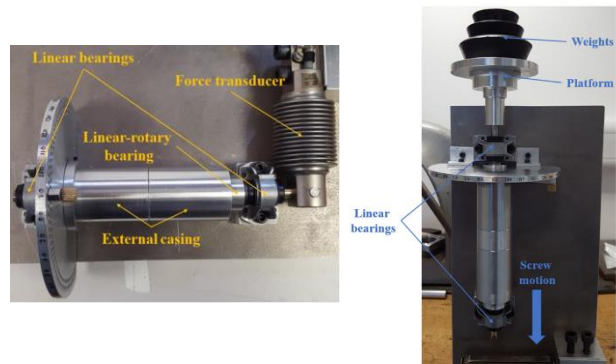

Fig. 17 Variation of Thrust force with relative linear displacement.

(a) method 1   (b) method 2
Fig. 18 Test-rig for force measurement